

Research Article

Preparation and Photocatalytic Activity of Ag Modified Ti-Doped-Bi₂O₃ Photocatalyst

Lilan Zhang, Junfeng Niu, Duo Li, Ding Gao, and Jianghong Shi

State Key Laboratory of Water Environment Simulation, School of Environment, Beijing Normal University, Beijing 100875, China

Correspondence should be addressed to Junfeng Niu; junfengn@bnu.edu.cn and Jianghong Shi; shijianghong@bnu.edu.cn

Received 15 December 2013; Accepted 8 January 2014; Published 17 February 2014

Academic Editor: Shaohua Shen

Copyright © 2014 Lilan Zhang et al. This is an open access article distributed under the Creative Commons Attribution License, which permits unrestricted use, distribution, and reproduction in any medium, provided the original work is properly cited.

Ti doped Bi₂O₃ (TDB) and Ag ion modified Ti doped Bi₂O₃ (Ag@TDB) photocatalysts were prepared by framework replacement synthesis method with different Ag loadings (0.05, 0.3, 0.75, and 1.0 mol/L AgNO₃). The structural properties of the prepared catalysts were studied by scanning electron microscope (SEM), X-ray diffraction (XRD), BET surface area, and UV/Vis diffuse reflectance (DRS). The XRD spectra of the Ti doped Bi₂O₃ calcined at 650°C showed the diffraction peaks of a mixture of Bi₁₂TiO₂₀ and Bi₄Ti₃O₁₂, with bits of mixed crystallite consisting of TiO₂ and Bi₂O₃. A high blue shift in the range 650–550 nm was detected in the DRS band. This blue shift increased with the decreasing Ag content. The photocatalytic activities of the catalysts were evaluated for the degradation of crystal violet (CV) under UV light irradiation. The results indicated that the degradation rate of CV by using 1.0 mol/L AgNO₃ doped bismuth titanate composite photocatalyst (1.0 Ag@TDB) was 1.9 times higher than that by using the bare Ti doped Bi₂O₃ photocatalyst. The higher activity of Ag@TDB is due to the enhancement of electron-hole pair separation by the electron trapping of silver particles.

1. Introduction

Photocatalytic degradation of organic pollutants is an alternative and harmless technology for the removal of organic impurities [1]. The crucial step for its application is to develop new, efficient, and clean catalysts. Recently, bismuth-based oxides photocatalysts such as Bi₂O₃, BiVO₄, and Bi₂WO₆ have attracted much attention due to their attractive photocatalytic properties under visible light irradiation [2–4]. Bi₂O₃ has been widely used in gas sensors, solid oxide fuel cells, optical coatings, and ceramic glass manufacturing due to its high refractive index, dielectric permittivity, marked photoluminescence properties, and thermal stability [5]. Furthermore, Bi₂O₃ has also shown higher photocatalytic activities in splitting water and decomposing pollutant. Despite the positive attributes of Bi₂O₃, low quantum yields hinder its practical application.

To improve the photocatalytic properties of catalysts, transition-metal ions with 3D electron structure, such as Fe(III), Sm(III), and Zn(II), have been widely used to modify the photocatalysts because they can act as shallow

charge traps [6–9]. In our previous research, transition-metal ion Ti(IV) doped bismuth-based oxides photocatalysts have been confirmed to show higher photocatalytic activity. The decolorization rates of crystal violet (CV) in aqueous solution with Ti(IV) doped Bi₂O₃ (TDB) have been proved to be double compared with that with bare Bi₂O₃ [10]. Pentachlorophenol could be also removed efficiently by using TDB, and its reductive dechlorination route under visible light irradiation was firstly revealed [11]. The removal ratios of pentachlorophenol and 2,4-dichlorophenol were 99.7% and 99.2%, respectively, by using TDB photocatalysis combined with laccase catalysis [12]. The results showed that Ti (IV)-doping improved the light absorption capacity and enhanced the photogenerated electron yield of Bi₂O₃, which was mainly attributed to the narrowed band gap (E_g) and red shift of light absorption edge [10].

The photocatalytic efficiency of catalysts is closely related to the rates of recombination of photoexcited electrons and holes [13]. Insertion of noble metal (e.g., Pt, Au, and Ag) could reduce the rate of charge carrier recombination and then improve the photocatalytic activity of catalysts. For example,

Sobana et al. [14] reported that the photocatalytic activity of silver doped TiO_2 was far much higher than that of the bare TiO_2 for the degradation of azo dyes. Additionally, the photonic efficiency of all metal-doped TiO_2 (i.e., Pt, Au, and Pd) was found to be higher than bare TiO_2 due to the acceleration of hydroxyl radical formation and decreasing recombination [15]. Rayalu et al. [16] used Au/TiO_2 as a catalyst in hydrogen generation under visible light illumination for their high photocatalytic activity. Evidence indicated that the photocatalytic activity could be enhanced by the impregnation of the semiconductor surfaces with optimal loading.

The aim of this study was to assess the photocatalytic activity of TDB by additional doping with Ag ion. A series of Ag ion modified Ti doped Bi_2O_3 (Ag@TDB) photocatalysts were prepared by the framework replacement synthesis method. The influences of the Ag ion contents on the surfacial properties, optical absorption, and crystal shape of the photocatalysts were studied. The photocatalytic degradation of CV was explored by using Ag@TDB , and the optimal Ag ion loading content was obtained. Finally, the promotion mechanisms of Ag@TDB were proposed.

2. Materials and Methods

2.1. Catalyst Preparation. The bare TDB was prepared by a hydrothermal synthesis technique as described in detail elsewhere [11]. The TDB photocatalysts were then dipped in an aqueous solution of silver nitrate (AgNO_3) with proper concentration after 2 h of illumination under UV light (at 254 nm) from a G15W/T8 Sylvania tube lamp (in the presence of atmospheric oxygen). After dipping, the catalysts were thoroughly washed with ultrapure water and dried at 150°C for 24 h. The concentrations of AgNO_3 were 0.05, 0.3, 0.75, and 1.0 mol/L. The prepared photocatalysts were labeled as 0.05 Ag@TDB , 0.3 Ag@TDB , 0.75 Ag@TDB , and 1.0 Ag@TDB , respectively.

2.2. Catalyst Characterization. Detailed surface images of the photocatalysts were obtained by means of a scanning electron microscope (SEM, JSM-6360LV, Hitachi). The structures of the photocatalysts were characterized by X-ray diffraction (XRD, D/MAX-rb, Rigaku). UV-visible absorbance spectrophotometry (DRS, Varian-CARY 1E UV-visible spectrophotometer, Varian) was used to measure the absorption spectrometry. The surface area and pore sizes were measured using a gas sorption analyzer (ASAP-2010 M, Micromeritics).

2.3. Photocatalytic Degradation of Crystal Violet. The photocatalytic efficiencies of catalysts were evaluated by the degradation of CV in aqueous solution. In all cases, a volume of 100 mL CV solution was used to conduct the photocatalytic experiments with regard to the effects of catalyst dosages (0.2 g/L, 1.0 g/L, 1.6 g/L, and 2.0 g/L), catalyst types (TDB, 0.05 Ag@TDB , 0.3 Ag@TDB , 0.75 Ag@TDB , and 1.0 Ag@TDB), and initial CV concentrations (5, 10, 20 mg/L). The dye solution containing the appropriate quantity of the photocatalyst powder was magnetically stirred before and during

illumination. Prior to irradiation, the suspension solution was firstly ultrasonicated for 15 min and then transferred to the photocatalytic reactor. The reactor was covered by aluminium foil to prevent UV light leakage. The suspension was irradiated under an 8 W UV lamp (UV354L, 354 nm, Beony S.T.). A suspension solution of 5 mL was withdrawn after periodic interval of irradiation and analyzed after filtration. The photocatalytic degradation ratio of CV was monitored by measuring the absorbance in a UV-Vis spectrophotometer.

3. Results and Discussion

3.1. Characterization. The phase and composition of TDB photocatalysts were characterized by XRD. Figure 1(a) shows the XRD pattern of the bare TDB photocatalyst. The diffraction peaks can be indexed to a mixture of $\text{Bi}_{12}\text{TiO}_{20}$ and $\text{Bi}_4\text{Ti}_3\text{O}_{12}$, with bits of mixed crystallite consisting of TiO_2 and Bi_2O_3 . The monoclinic phase was mixed with three-phase (α , β , γ). Bismuth-based oxides exist in four stable crystalline phases under atmospheric pressure: α , β , γ , and δ [17]. The crystalline phase significantly affects the structural, textural, and catalytic properties of photocatalyst [10].

The prepared TDB catalysts show light yellow colors. Dipping the TDB catalysts in AgNO_3 aqueous could darken the particles, revealing the presence of silver compounds [18, 19]. In order to explore the influence of Ag ion doping on the optic absorption of photocatalysts, a UV-Vis spectrophotometer was used to measure their absorption spectra with the wavelength from 240 to 800 nm. As shown in Figure 1(b), all the catalysts have good properties of visible light absorption. The absorption peak of TDB even extends to >500 nm. Comparably, the absorption peaks of all the Ag@TDB catalysts have blue shift phenomenon. In particular, the photocatalyst 1.0 Ag@TDB exhibits an absorption peak at 450 nm. The degree of blue shifting of catalysts decreased with the increase of the Ag ion content in the catalysts. The blue shift in the UV absorption spectra has been also reported in ceria-containing nanomaterials in recent years, and the quantum size effect has been proposed to explain this phenomenon for the pure ceria nanocrystals [20, 21]. Considering the blue shift in the UV spectra for the Ag@TDB system, the energy level lied beneath the valence band formed by the hybrid track of Bi 6s and O 2p for the bare TDB. The impurity levels of Ag@TDB were located between valence band and conduction band of TDB due to Ag ion doping, which potentially led to the blue shift. This phenomenon was not convenient for visible light absorption but for photocatalytic reactions under UV light illumination.

The morphology of the photocatalysts was characterized by SEM. Figure 2 reveals that particle diameters ranging from 80 to 200 nm varied in size and shape. These particles were easy to cluster into aggregates ranging from 5 to 200 μm , and their shapes were mostly spherical and ellipsoidal in the low-resolution image. Compared with the TDB, the shape of the Ag@TDB changed from duct-like to scale-like and then into slice with the increasing Ag ion content from 0.05 to 1.0 mol/L. The morphology of the photocatalyst is closely related to their activities [2]. The Brunauer Emmett Teller

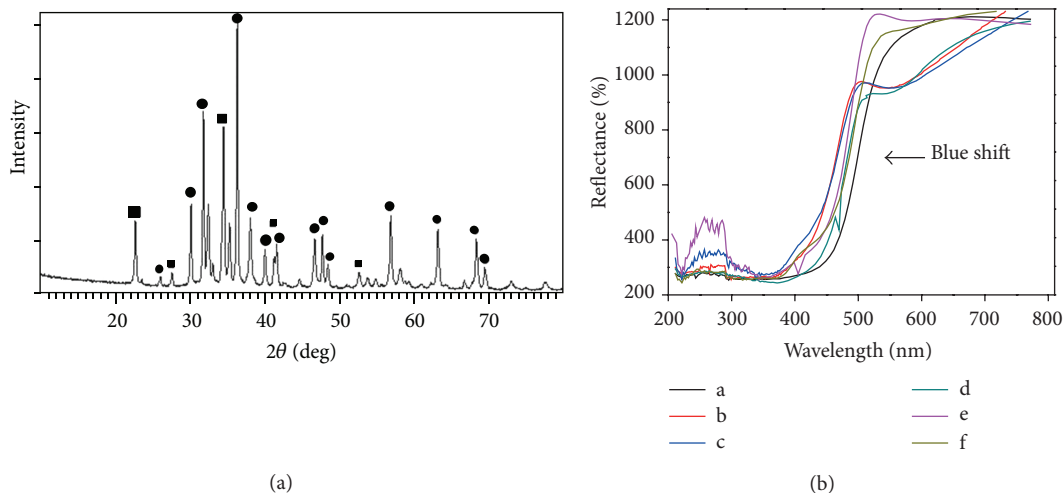


FIGURE 1: (a) Powder X-ray diffraction (XRD) patterns of bismuth titanate composite; ● represents the XRD peak of $\text{Bi}_{12}\text{Ti}_{20}$; ■ represents the XRD peak of $\text{Bi}_4\text{Ti}_3\text{O}_{12}$. (b) UV-Vis diffuse reflectance spectra of TDB—a; 0.05 Ag@TDB—b; 0.1 Ag@TDB—c; 0.3 Ag@TDB—d; 0.75 Ag@TDB—e; and 1.0 Ag@TDB—f.

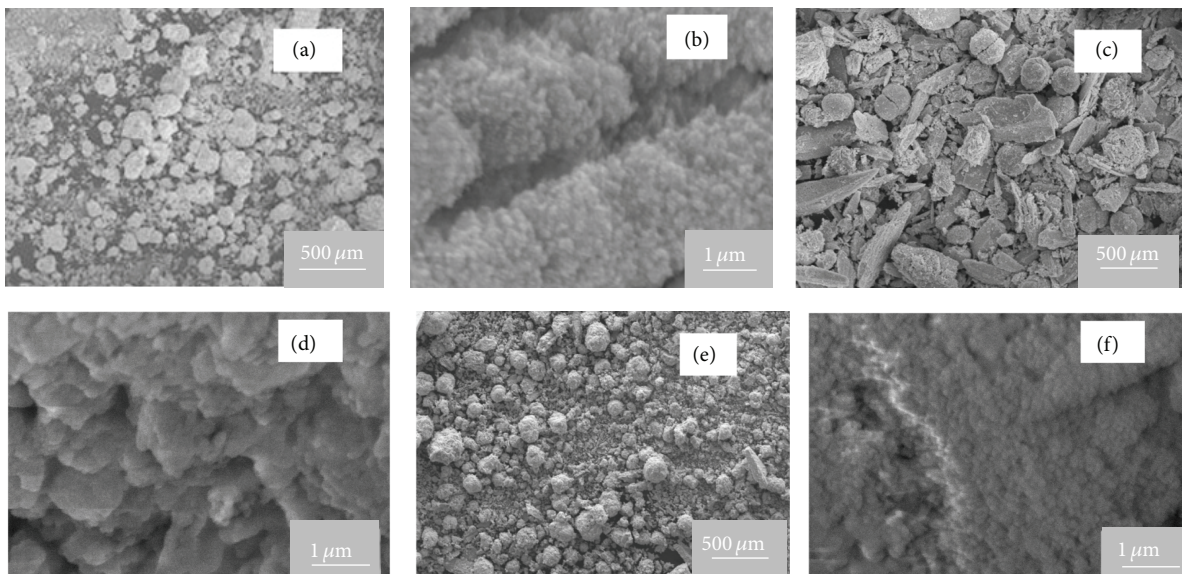


FIGURE 2: Scanning electron microscopy images of photocatalyst with bismuth titanate composite (TDB) without Ag-dope (a), (b); 0.05 Ag@TDB (c), (d); and 1.0 Ag@TDB (e), (f) with image resolution at 500 μm and 1 μm .

(BET) surface areas of the photocatalysts were 20~60 m^2/g . There was no significant change in the surface area after metallisation of TDB particles. The average pore size estimated by the Barrett Joyner Halenda (BJH) method was 1.7 nm, indicating that these catalysts have mesoporous structure and good photocatalytic performances.

3.2. Evaluation of the Photocatalytic Activity

3.2.1. *Effect of Catalyst Concentration.* To remove pollutants economically and efficiently, it is important to find the optimal amount of catalyst. The effect of photocatalyst TDB concentration from 0.2 to 2.0 g/L on the photodegradation of

CV solution of 5 mg/L was explored under UV irradiation under room temperature. As shown in Figure 3, the degradation rates increased from 0.335 to 0.47 with the increase of the catalyst dosage from 0.2 to 1.0 g/L. The degradation rate was almost constant when the dosage of the catalyst was beyond 1.0 g/L. At the low catalyst concentration, the increase of TDB particle concentrations led to the increase of the number of absorbed photons and the number of the adsorbed dye molecules, enhancing the photocatalytic efficiency. As the concentration of catalyst was higher than the optimal value, the degradation rates decreased due to the increasing turbidity of the suspension and light scattering. Hence, 1.0 g/L was used as the catalyst dosage for the following photocatalytic reactions.

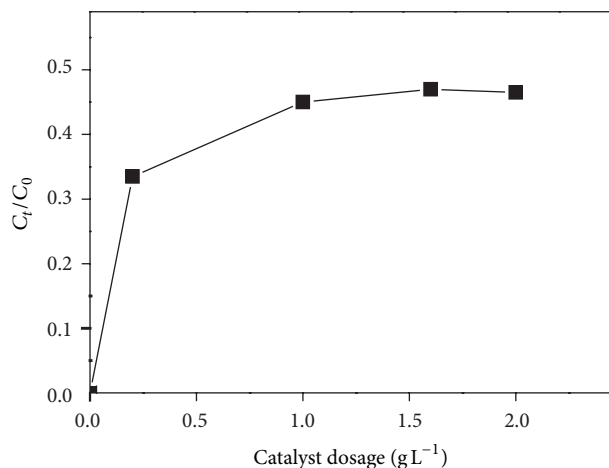


FIGURE 3: Effect of the TDB catalyst amount on degradation rate of crystal violet.

3.2.2. Effect of Initial Crystal Violet Concentration. The effect of initial CV concentration on the degradation efficiency was investigated by changing the initial concentration from 5.0 to 20.0 mg/L at constant catalyst loading (1.0 Ag@TDB, 1.0 g/L). The results are shown in Figure 4. The degradation rate of CV at low concentration was high. The degradation ratio decreased from 92.1% to 45.0% with the increase of initial CV concentration from 5 mg/L to 20 mg/L, suggesting that the increase of the dye concentration decreased the removal ratio. Similar results have been reported for the photocatalytic degradation of other dyes in aqueous solution (e.g., quinolone yellow, acid red, and reactive dyes 4) [22–24]. An explanation to this phenomenon was that the increase of dye concentration led to the increase of the amount of dye adsorbed on the catalyst surface, reducing the active sites for adsorption of hydroxyl ions and the generation of hydroxyl radicals. The increase of dye concentration could also intercept the path of photons reaching the catalyst surface and decrease the adsorption of photons on catalyst particles. Additionally, at high concentration, the dye molecules would compete for UV light absorption with the catalyst, which may also reduce the degradation efficiency [25].

3.2.3. Effect of Catalysts Type. The photocatalytic activities of TDB and Ag@TDB were evaluated and compared by degradation of CV at 5 mg/L in aqueous solution under UV light irradiation. As shown in Figure 5, the removal rate of CV is below 5% in the dark, indicating that the adsorption of catalysts could be negligible. The removal ratio of CV was 33.5% by using TDB photocatalyst in 80 min. Under the same reaction conditions, the removal ratios of CV were 36.1%, 62.5%, 86.64%, and 91.5% by using 0.05 Ag@TDB, 0.3 Ag@TDB, 0.75 Ag@TDB, and 1.0 Ag@TDB photocatalysts, respectively. The results indicated that all the Ag modified particles exhibited higher activities than the bare TDB particles. The degradation rate of CV increased with the increase of the Ag ion doping content. The main reason might be that Ag ions on Ag@TDB surface acted as sites where electrons

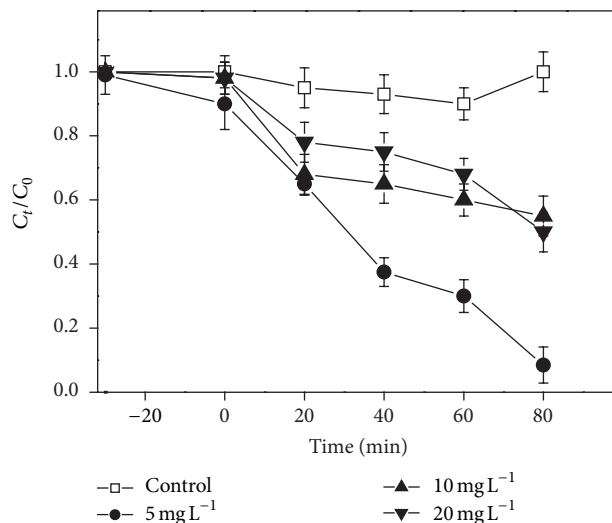


FIGURE 4: Crystal violet concentration change as a function of photocatalysis time at initial concentration of 5, 10, and 20 mg/L with 1.0 g/L Ag@TDB catalyst.

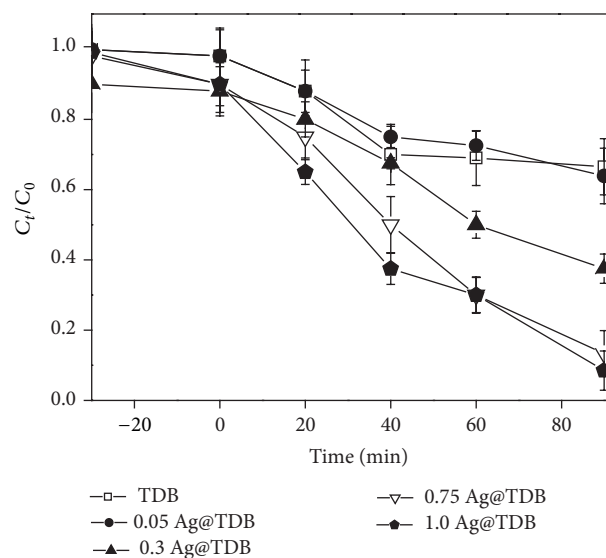


FIGURE 5: Degradation of crystal violet at 5.0 mg L⁻¹ with different Ag ion doping TDB under UV light irradiation.

accumulated. Better separation of electrons and holes on Ag@TDB catalyst surface allowed more efficient channeling of the charge carriers into useful reduction and oxidation reactions rather than recombination reactions [26, 27]. The degradation rate with 0.75 Ag@TDB was 1.4 times that with 0.05 Ag@TDB. The degradation rate with 1.0 Ag@TDB was only 0.05 times that with 0.75 Ag@TDB. This change can be due to the fact that Ag particles can act as recombination centers as the Ag content is beyond its optimal value [27, 28]. Furthermore, the active sites of catalyst were fully occupied by Ag ions. The rest of Ag ions played slight role on CV degradation, leading to slight rise of CV degradation rate with higher Ag ion doping. Additionally, it was observed that

the color of catalyst became darker during the irradiation. The main reason was that the reduction potential of silver ion is prone to photocatalytic reduction $\text{Ag}^+ + \text{e}^- \rightarrow \text{Ag}^0$, producing metallic silver on catalyst surface.

4. Conclusions

The doping of silver alters the structure of TDB catalyst and leads to the blue shift. The degradation ratios of CV were obtained by using TDB and Ag@TDB photocatalysts in aqueous solution under UV light irradiation. The results indicated that the degradation efficiency of CV was significantly impacted by its initial concentrations, photocatalyst amounts, and photocatalyst types. The optimal amount of photocatalyst was 1.0 g/L at the CV concentration of 5 mg/L. For photocatalyst type, the photocatalytic activities of Ag@TDB were significantly higher than those of bare TDB. There are two main reasons: (1) Ag ion doped improved the photocatalyst activities due to trapping photoelectrons of Ag ion and (2) the photocatalyst has mesoporous structure. CV could be effectively degraded by Ag@TDB under UV light irradiation, indicating that Ag@TDB is expected to exhibit high practicability and good performance for the degradation of dyes.

Conflict of Interests

The authors declare that there is no conflict of interests regarding the publication of this paper.

Acknowledgments

This study was financially supported by the National Natural Science Foundation of China (no. 21077010), the Fok Ying-Tong Education Foundation of China (Grant no. 121077), and the Specialized Research Fund for the Doctoral Program of Higher Education of China (no. 201110003110023).

References

- [1] D. S. Bhatkhande, V. G. Pangarkar, and A. A. Beenackers, "Photocatalytic degradation for environmental applications—a review," *Journal of Chemical Technology and Biotechnology*, vol. 77, no. 1, pp. 102–116, 2002.
- [2] M. Shang, W. Wang, L. Zhang, S. Sun, L. Wang, and L. Zhou, "3D $\text{Bi}_2\text{WO}_6/\text{TiO}_2$ hierarchical heterostructure: controllable synthesis and enhanced visible photocatalytic degradation performances," *Journal of Physical Chemistry C*, vol. 113, no. 33, pp. 14727–14731, 2009.
- [3] T. Saison, N. Chemin, C. Chaneéac et al., " Bi_2O_3 , BiVO_4 , and Bi_2WO_6 : impact of surface properties on photocatalytic activity under visible light," *Journal of Physical Chemistry C*, vol. 115, no. 13, pp. 5657–5666, 2011.
- [4] S. Anandan, G.-J. Lee, P.-K. Chen, C. Fan, and J. J. Wu, "Removal of Orange II dye in water by visible light assisted photocatalytic ozonation using Bi_2O_3 and $\text{Au}/\text{Bi}_2\text{O}_3$ nanorods," *Industrial and Engineering Chemistry Research*, vol. 49, no. 20, pp. 9729–9737, 2010.
- [5] M.-S. Gui, W.-D. Zhang, Q.-X. Su, and C.-H. Chen, "Preparation and visible light photocatalytic activity of $\text{Bi}_2\text{O}_3/\text{Bi}_2\text{WO}_6$ heterojunction photocatalysts," *Journal of Solid State Chemistry*, vol. 184, no. 8, pp. 1977–1982, 2011.
- [6] X. H. Wu, W. Qin, L. Li, Y. Guo, and Z. Y. Xie, "Photocatalytic property of nanostructured Fe^{3+} -doped Bi_2O_3 films," *Catalysis Communications*, vol. 10, no. 5, pp. 600–604, 2009.
- [7] J. K. Reddy, B. Srinivas, V. D. Kumari, and M. Subrahmanyam, " Sm^{3+} -doped Bi_2O_3 photocatalyst prepared by hydrothermal synthesis," *ChemCatChem*, vol. 1, no. 4, pp. 492–496, 2009.
- [8] A. Hameed, V. Gombac, T. Montini, L. Felisari, and P. Fornasiero, "Photocatalytic activity of zinc modified Bi_2O_3 ," *Chemical Physics Letters*, vol. 483, no. 4–6, pp. 254–261, 2009.
- [9] R. J. Tayade, R. G. Kulkarni, and R. V. Jasra, "Transition metal ion impregnated mesoporous TiO_2 for photocatalytic degradation of organic contaminants in water," *Industrial and Engineering Chemistry Research*, vol. 45, no. 15, pp. 5231–5238, 2006.
- [10] L. Yin, J. Niu, Z. Shen, and Y. Sun, "The electron structure and photocatalytic activity of Ti(IV) doped Bi_2O_3 ," *Science China Chemistry*, vol. 54, no. 1, pp. 180–185, 2011.
- [11] L. Yin, J. Niu, Z. Shen, and J. Chen, "Mechanism of reductive decomposition of pentachlorophenol by Ti-doped $\beta\text{-Bi}_2\text{O}_3$ under visible light irradiation," *Environmental Science and Technology*, vol. 44, no. 14, pp. 5581–5586, 2010.
- [12] L. Yin, Z. Shen, J. Niu, J. Chen, and Y. Duan, "Degradation of pentachlorophenol and 2,4-dichlorophenol by sequential visible-light driven photocatalysis and laccase catalysis," *Environmental Science and Technology*, vol. 44, no. 23, pp. 9117–9122, 2010.
- [13] U. I. Gaya and A. H. Abdullah, "Heterogeneous photocatalytic degradation of organic contaminants over titanium dioxide: a review of fundamentals, progress and problems," *Journal of Photochemistry and Photobiology C*, vol. 9, no. 1, pp. 1–12, 2008.
- [14] N. Sobana, M. Muruganadham, and M. Swaminathan, "Nano-Ag particles doped TiO_2 for efficient photodegradation of Direct azo dyes," *Journal of Molecular Catalysis A*, vol. 258, no. 1–2, pp. 124–132, 2006.
- [15] S. Sakthivel, M. V. Shankar, M. Palanichamy, B. Arabindoo, D. W. Bahnemann, and V. Murugesan, "Enhancement of photocatalytic activity by metal deposition: characterisation and photonic efficiency of Pt, Au and Pd deposited on TiO_2 catalyst," *Water Research*, vol. 38, no. 13, pp. 3001–3008, 2004.
- [16] S. S. Rayalu, D. Jose, M. V. Joshi, P. A. Mangrulkar, K. Shrestha, and K. Klabunde, "Photocatalytic water splitting on Au/TiO_2 nanocomposites synthesized through various routes: enhancement in photocatalytic activity due to SPR effect," *Applied Catalysis B*, vol. 142–143, pp. 684–693, 2013.
- [17] N. M. Sammes, G. A. Tompsett, H. Näfe, and F. Aldinger, "Bismuth based oxide electrolytes—structure and ionic conductivity," *Journal of the European Ceramic Society*, vol. 19, no. 10, pp. 1801–1826, 1999.
- [18] I. M. Arabatzis, T. Stergiopoulos, M. C. Bernard, D. Labou, S. G. Neophytides, and P. Falaras, "Silver-modified titanium dioxide thin films for efficient photodegradation of methyl orange," *Applied Catalysis B*, vol. 42, no. 2, pp. 187–201, 2003.
- [19] T. Sano, N. Negishi, D. Mas, and K. Takeuchi, "Photocatalytic Decomposition of N_2O on Highly Dispersed Ag+ Ions on TiO_2 Prepared by Photodeposition," *Journal of Catalysis*, vol. 194, no. 1, pp. 71–79, 2000.
- [20] L. Yin, Y. Wang, G. Pang, Y. Kolytyn, and A. Gedanken, "Sonochemical synthesis of cerium oxide nanoparticles—effect

- of additives and quantum size effect," *Journal of Colloid and Interface Science*, vol. 246, no. 1, pp. 78–84, 2002.
- [21] R. Si, Y.-W. Zhang, C.-X. Xiao et al., "Non-template hydrothermal route derived mesoporous $\text{Ce}_{0.2}\text{Zr}_{0.8}\text{O}_2$ nanosized powders with blue-shifted UV absorption and high CO conversion activity," *Physical Chemistry Chemical Physics*, vol. 6, no. 5, pp. 1056–1063, 2004.
- [22] Y. Peng, J. Ji, X. Zhao, H. Wan, and D. Chen, "Preparation of ZnO nanopowder by a novel ultrasound assisted non-hydrolytic sol–gel process and its application in photocatalytic degradation of C.I. Acid Red 249," *Powder Technology*, vol. 233, pp. 325–330, 2013.
- [23] S. K. Sharma, H. Bhunia, and P. K. Bajpai, "Photocatalytic decolorization kinetics and adsorption isotherms of a mixture of two anionic azo dyes: Reactive Red 120 and Reactive Black 5," *Desalination and Water Treatment*, vol. 44, no. 1–3, pp. 261–268, 2012.
- [24] V. K. Gupta, R. Jain, S. Agarwal, A. Nayak, and M. Shrivastava, "Photodegradation of hazardous dye quinoline yellow catalyzed by TiO_2 ," *Journal of Colloid and Interface Science*, vol. 366, no. 1, pp. 135–140, 2012.
- [25] A. Mills, R. H. Davies, and D. Worsley, "Water purification by semiconductor photocatalysis," *Chemical Society Reviews*, vol. 22, no. 6, pp. 417–425, 1993.
- [26] S. Kohtani, J. Hiro, N. Yamamoto, A. Kudo, K. Tokumura, and R. Nakagaki, "Adsorptive and photocatalytic properties of Ag-loaded BiVO_4 on the degradation of 4-*n*-alkylphenols under visible light irradiation," *Catalysis Communications*, vol. 6, no. 3, pp. 185–189, 2005.
- [27] S. Rengaraj and X. Z. Li, "Enhanced photocatalytic activity of TiO_2 by doping with Ag for degradation of 2,4,6-trichlorophenol in aqueous suspension," *Journal of Molecular Catalysis A*, vol. 243, no. 1, pp. 60–67, 2006.
- [28] V. Vamathevan, R. Amal, D. Beydoun, G. Low, and S. McEvoy, "Photocatalytic oxidation of organics in water using pure and silver-modified titanium dioxide particles," *Journal of Photochemistry and Photobiology A*, vol. 148, no. 1–3, pp. 233–245, 2002.

